Electronic Supplementary Information

Metal center regulation of porphyrin unit in covalent organic polymer for boosting the photocatalytic CO_2 reduction activity†

Shengtao Chen,[a] Meijing Liao,[b] Xinming Li,[a] Renjie Li,[a] Jin Zhang,*[a] Yuexing Zhang*[b] and Tianyou Peng*[a]

[a] *College of Chemistry and Molecular Sciences, Engineering Research Center of Organosilicon Compounds & Materials, Wuhan University, Wuhan 430072, PR China*

[b] *College of Chemistry and Chemical Engineering, Hubei University, Wuhan 430062, PR China.*

* Corresponding authors.

E-mail: typeng@whu.edu.cn (T. Peng). ORCID: 0000-0002-2527-7634; jzhang@whu.edu.cn (J. Zhang); zhangyuexing@sdu.edu.cn (Y. Zhang).

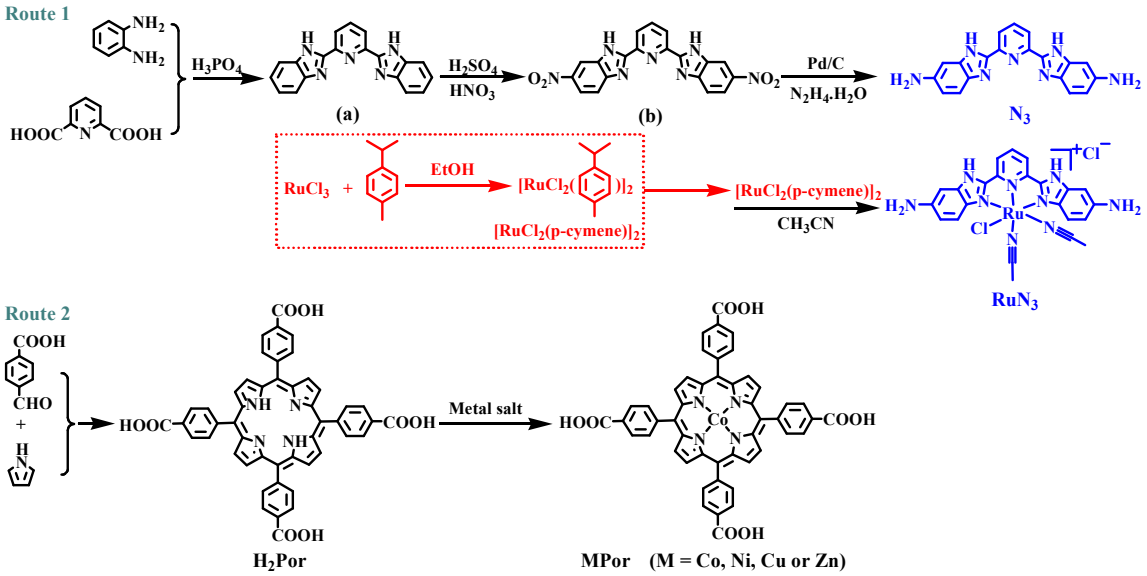

Scheme S1 Synthetic routes of 2,6-bis(5-amino-benzimidazol-2-yl)pyridine Ru(II) pincer complex (RuN_3) monomer and *meso*-tetrakis(4-chlorobenzoyl)porphyrin (MPor, M = H_2, Co, Ni, Cu or Zn) monomers.

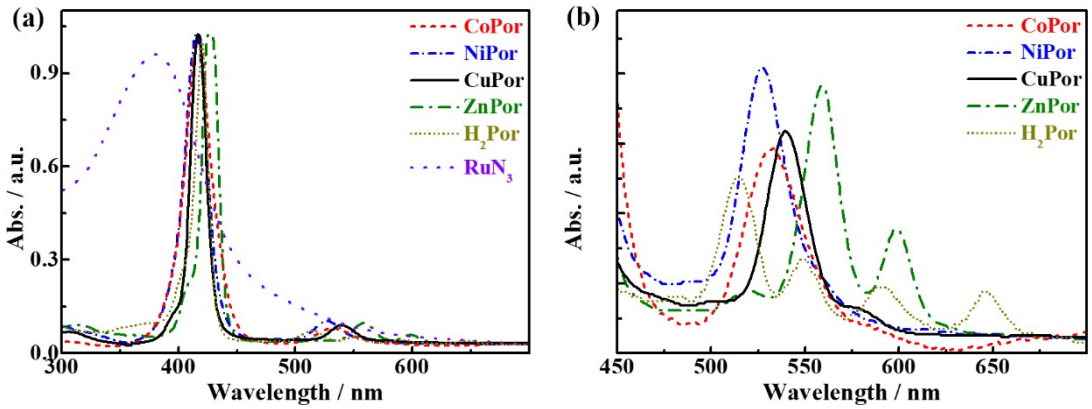

Fig. S1 (a) UV-Vis absorption spectra of the MPor and RuN_3 monomers. (b) Enlarged UV-Vis absorption spectra in the range of 450-700 nm of the MPor monomers.

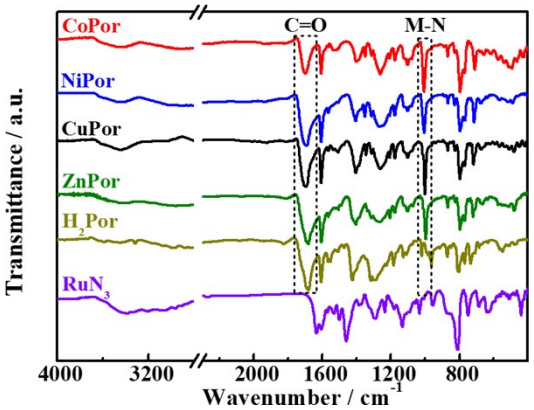

Fig. S2 FT-IR spectra of the MPor and RuN_3 monomers.

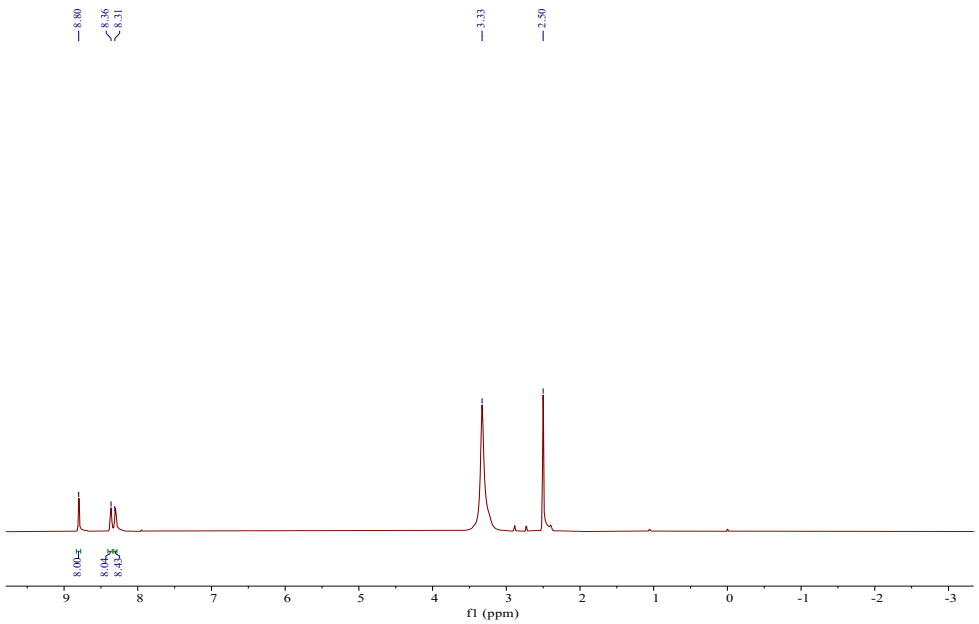

Fig. S3 ^{1}H NMR (DMSO-d_6) spectrum of the ZnPor monomer.

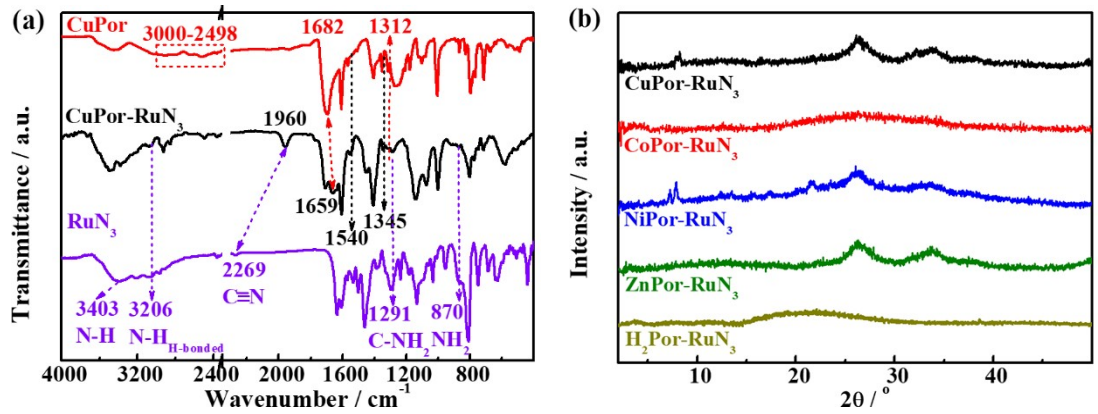

Fig. S4 (a) FT-IR spectra of the CuPor-RuN$_3$ COP and its monomers (CuPor and RuN$_3$). (b) XRD patterns of the MPor-RuN$_3$ COPs.

Table S1 Elemental analysis results of the MPor-RuN$_3$ COPs.*

Polymer	C (%)	H (%)	N (%)	M[a] (%)	Ru[a] (%)
CoPor-RuN$_3$	57.28 (57.37)	3.31 (3.26)	15.51 (15.67)	2.76 (3.00)	9.51 (10.30)
NiPor-RuN$_3$	57.51 (57.35)	3.27 (3.25)	15.42 (15.66)	3.17 (3.00)	9.91 (10.30)
CuPor-RuN$_3$	57.46 (57.21)	3.29 (3.25)	15.38 (15.62)	3.11 (3.20)	9.72 (10.20)
ZnPor-RuN$_3$	57.29 (57.16)	3.30 (3.24)	15.35 (15.61)	3.06 (3.30)	9.63 (10.20)
H$_2$Por-RuN$_3$	58.89 (59.03)	3.61 (3.45)	16.07 (16.21)	--	9.84 (10.60)

* Data in parentheses are theoretic ones calculated using following formula: MPor-RuN$_3$: [1*(MPor) + 2*(RuN$_3$) 4*(H$_2$O)] /3 = $C_{31.3}H_{21.3}N_{7.3}O_{1.3}Ru_{2/3}M_{1/3}Cl_{1.3}$; H$_2$Por-RuN$_3$: [1*(H$_2$Por) + 2*(RuN$_3$) - 4*(H$_2$O)]/3 = $C_{31.3}H_{22}O_{1.3}Ru_{2/3}Cl_{1.3}$.

[a] Metal contents were determined using an IRIS Intrepid II XSP inductively coupled plasma-atomic emission spectrometry (ICP-AES).

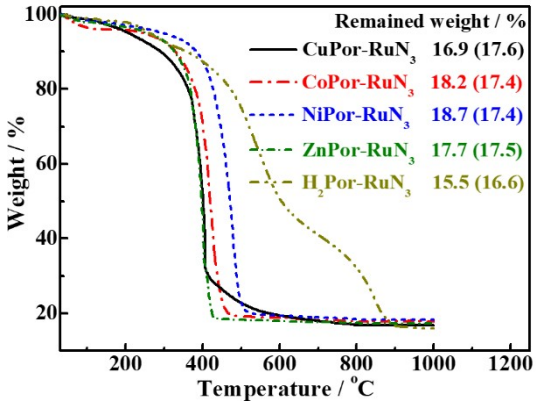

Fig. S5 TG curves of the MPor-RuN$_3$ COPs in air. Insets are the remained weight percentages, whereby the data in parentheses are the corresponding theoretic values calculated according to their respective formula shown in Table S1.

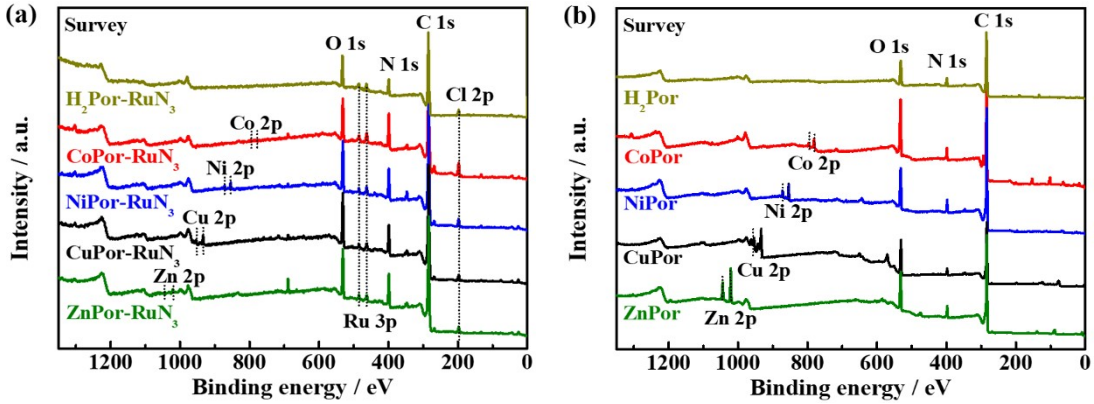

Fig. S6 Survey XPS spectra of the MPor-RuN$_3$ COPs (a) and their corresponding MPor monomers (b).

Table S2 Band positions of UV-vis absorption spectra of the MPor monomers and MPor-RuN$_3$ COPs

MPor	B-band / nm	Q-band / nm	MPor-RuN$_3$ COP	B-band / nm	Q-band / nm
H_2Por	420	515, 549, 591, 646	H_2Por-RuN$_3$	~472	519, 555, 592, 647
CoPor	417	532, 575	CoPor-RuN$_3$	~464	550, 601
NiPor	415	527	NiPor-RuN$_3$	~469	529
CuPor	417	540, 578	CuPor-RuN$_3$	~441	543, 594
ZnPor	427	524, 559, 599	ZnPor-RuN$_3$	457	524, 562, 606, 652

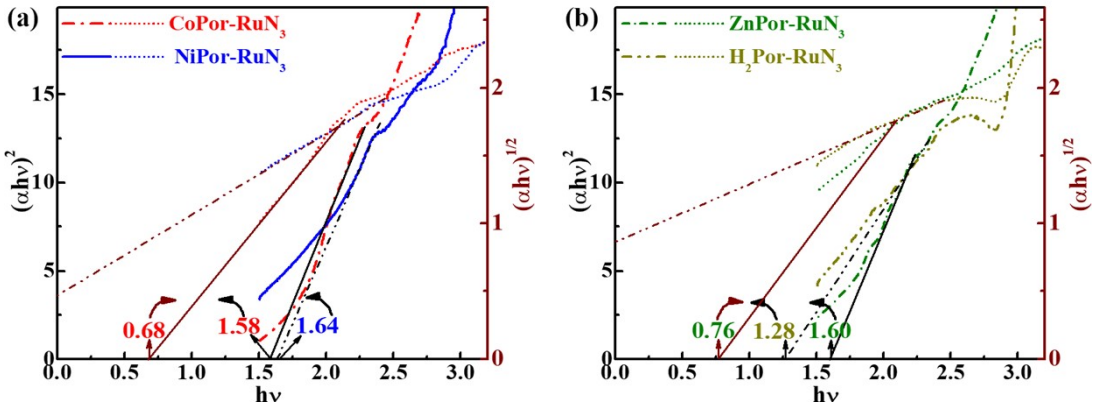

Fig. S7 $(\alpha h\nu)^2$ [or $(\alpha h\nu)^{1/2}$] *vs.* hν plots derived from the corresponding DRS spectra of the MPor-RuN$_3$ COPs. Obviously, it is more reasonable to calculate the optical band gaps with the $(\alpha h\nu)^2$ *vs.* hν plots.

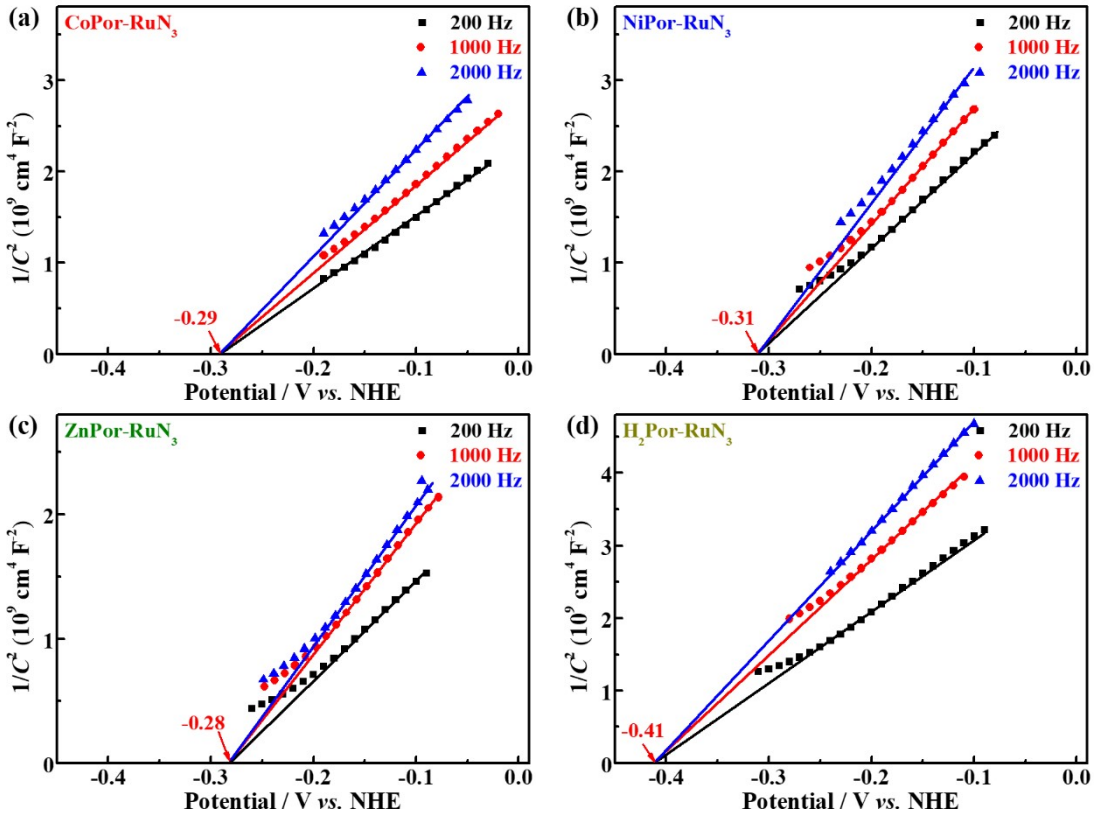

Fig. S8 Mott-Schottky plots of the MPor-RuN$_3$ COPs.

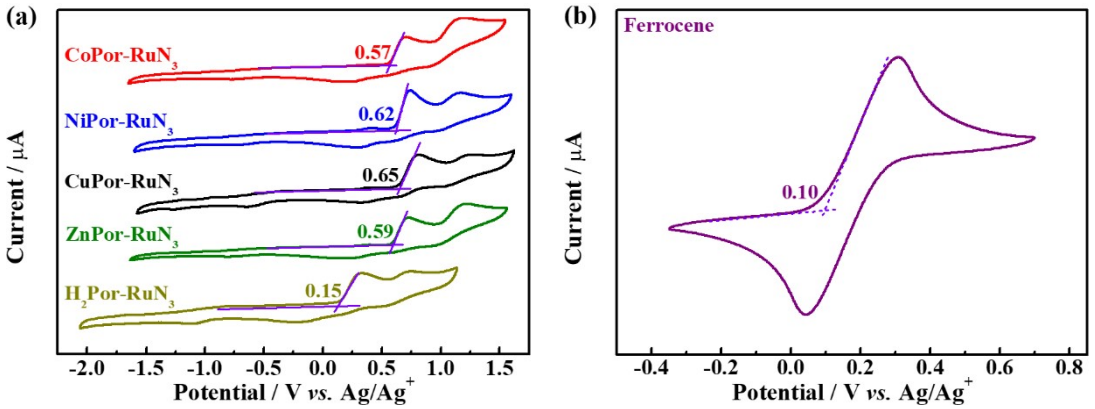

Fig. S9 Cyclic voltammogram (CV) plots of the MPor-RuN$_3$ COPs (a) and ferrocene reference (b).

Table S3 Electrochemical properties and energy band levels of MPor-RuN_3 COPs

Sample	E_g / eV	E_{CB} / V *vs.* NHE	E_{VB} / V *vs.* NHE	E_{HOMO} / V *vs.* NHE
CuPor-RuN_3	1.69	-0.42	1.27	1.29
CoPor-RuN_3	1.58	-0.39	1.19	1.21
NiPor-RuN_3	1.64	-0.41	1.24	1.26
ZnPor-RuN_3	1.60	-0.38	1.22	1.23
H_2Por-RuN_3	1.28	-0.51	0.77	0.79

Table S4 Summary of CO_2RR performances of various polymer-, MOF- or COF-based photocatalysts

Catalyst	Sacrificial agent	Solvent	λ (nm)	CO yield / μmol g^{-1} h^{-1}	CO selectivity / %	*Ref.*
MIL-101-Cr-EN	TEOA	CH_3CN	200-850	47.2	96.5	1
OXD-TPA	H_2O	H_2O	≥ 420	37.15	~100	2
MOF-525-Co	TEOA	CH_3CN	400-800	200.6	85.4	3
Ag⊂Re3-MOF-16 nm	TEA	CH_3CN/H_2O	400-700	0.098	--	4
ZrPP-1-Co	TEOA	CH_3CN	≥ 420	14	96.4	5
Re/Bp-PMO	TEOA	CH_3CN	≥ 280	25.8	--	6
PEosinY-1	--	H_2O	≥ 420	33	92	7
TTCOF-Zn/Ni/Cu	--	H_2O	420-800	2.06/0.08/1.44	~100	8
TAPBB-COF	--	H_2O	200-1000	24.6	95.6	9
Ru-MOF	TEOA	CH_3CN	420-800	67.5 ($HCOO^-$)	--	10
Co-POM	TEOA	CH_3CN	400-800	17.0	80	11
BIF-20@g-C_3N_4	TEOA	CH_3CN	400-800	53.9	77.6	12
Au-NC@UiO-68-NHC	CH_3OH	CH_3CN	300-800	57.6	84	13
UiO-66/CNNS	TEOA	CH_3CN	400-800	9.9	100	14
Pt/NH_2-MIL-125(Ti)	TEOA	CH_3CN	420-800	32.4 ($HCOO^-$)	100	15
Pt@NH_2-UiO-68	TEOA	--	400-780	66.7	100	16
Au/PPF-3	C_2H_5OH	CH_3CN	≥ 400	42.7 ($HCOO^-$)	100	17
UiO-68-OCH_3	TEOA	--	400-780	19.7	--	18
CPOP-30-Re	TEOA	CH_3CN	≥ 390	623	97.8	19
Re-Bpy-sp^2c-COF	TEOA	CH_3CN	≥ 420	1040	81	20
Cp*Rh@PerBpyCMP	TEOA,BIH	CH_3CN	420-950	700	100	21
CoPcPDA-CMP NSs	H_2O	--	≥ 400	14.27	92	22
Co@COP-30	TEOA	H_2O, CH_3CN	≥ 400	506	94	23
ZnPor@Re	BIH	DMF, TEOA	400-800	1379	99.8	24
PQD/PES	H_2O	--	AM1.5G	32.45	--	25
POSS-Re-2	BIH	DMF, TEOA	≥ 400	218.2	33.8	26
CoPor-RuN_3 COP	BIH	DMF	≥ 400	37.1	96	27
CuPor-RuN_3 COP	BIH	CH_3CN	400-850	74.3	100	This
CuPor-RuN_3 COP	BIH	CH_3CN	300-850	143.7	100	work

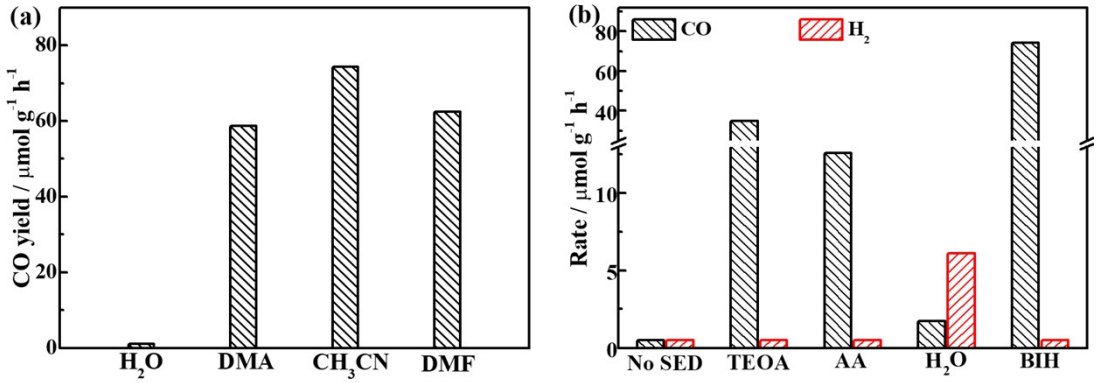

Fig. S10 Effects of solvents (a) and sacrificial electron donors (b) on the photocatalytic CO_2RR activity of the CuPor-RuN_3 COP under visible light ($\lambda \geq 400$ nm) irradiation.

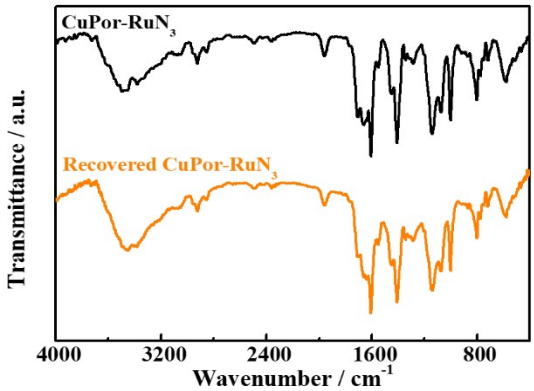

Fig. S11 FT-IR spectra of the CuPor-RuN_3 COP before and after the 20 h photoreaction.

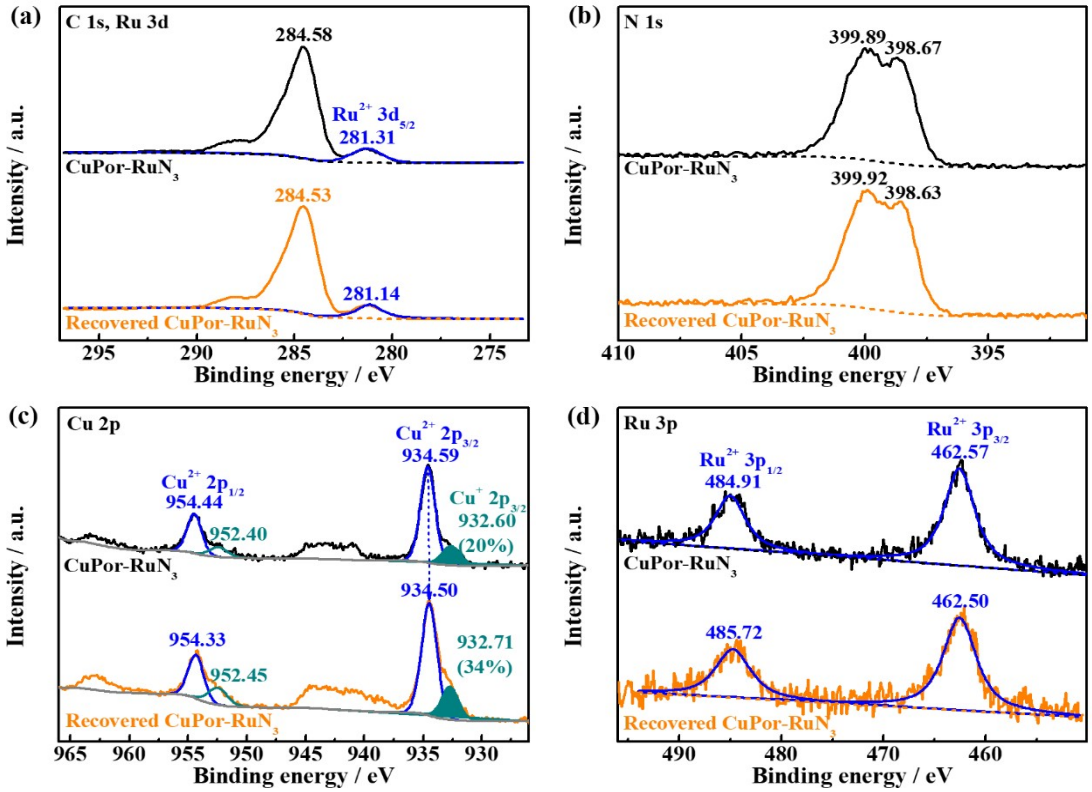

Fig. S12 High-resolution XPS spectra of the CuPor-RuN_3 COP before and after the 20 h photoreaction. (a) C 1s & Ru 3d, (b) N 1s, (c) Cu 2p, (d) Ru 3p.

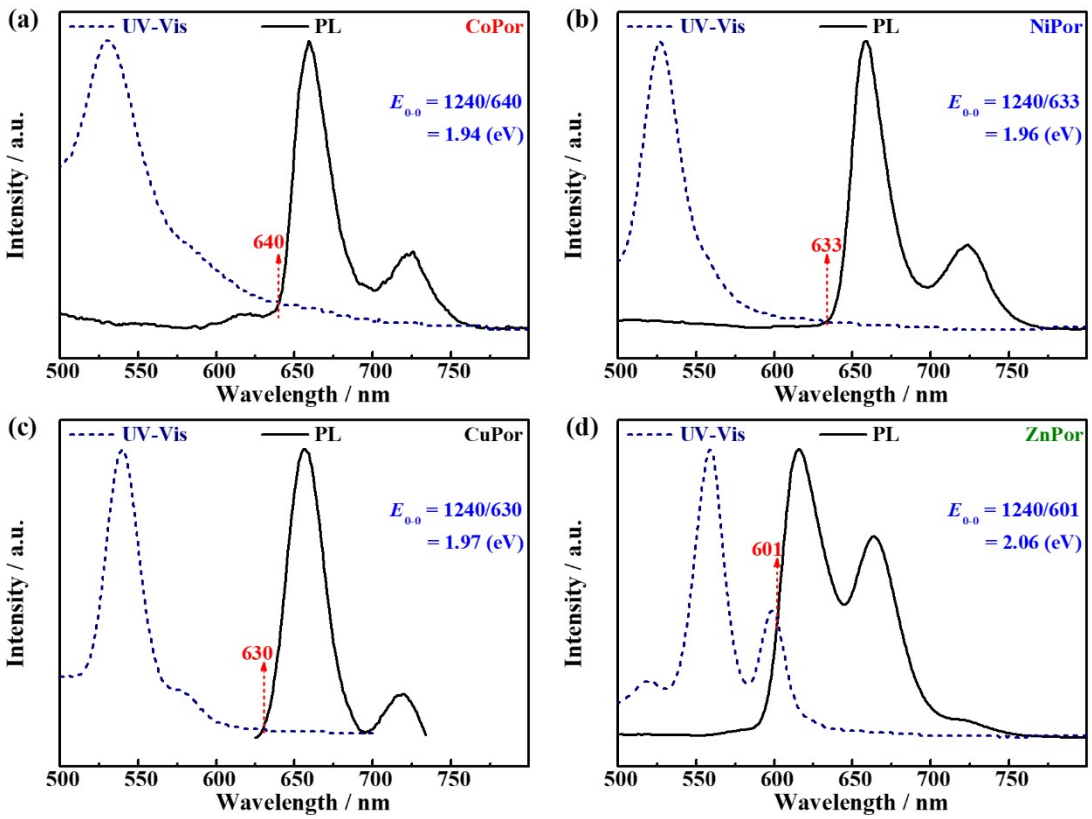

Fig. S13 Normalized emission/absorption spectra of various MPor monomers at λ_{ex} = 415 nm.

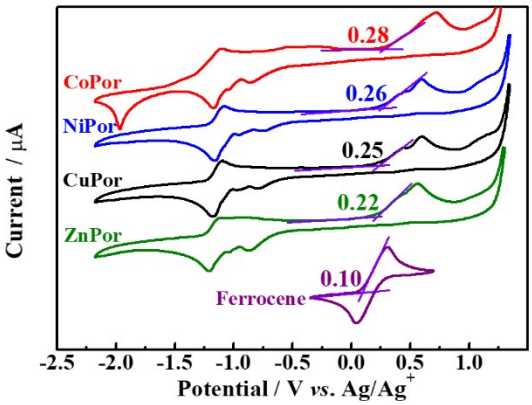

Fig. S14 CV plots of various MPor monomers and ferrocene reference.

The highest occupied molecular orbital (HOMO)-lowest unoccupied molecular orbital (LUMO) gap energies ($E_{0\text{-}0}$) of MPor monomers can be estimated by the intersection point between their normalized absorption and emission spectra (Fig. S13) according to equation of $E_{0\text{-}0}$ (eV) = 1240/λ (nm). The oxidation potentials (E) of ground-state monomers can be determined using cyclic voltammogram (CV) curves with ferrocene redox pair (Fc^+/Fc) as reference (Fig. S14). Therefore, the E_{HOMO} and E_{LUMO} levels of those MPor monomers can be calculated using Eqs. 1 and 2.

$$E_{HOMO} = E_{OX} \text{ (V } vs. \text{ Ag/Ag}^+) - E_{1/2}(Fc^+/Fc \text{ } vs. \text{ Ag/Ag Ag}^+) + E_{1/2}(Fc^+/Fc \text{ } vs. \text{ NHE}) \quad (1)$$

$$E_{LUMO} = (E_{HOMO} - E_{0\text{-}0}) \quad (2)$$

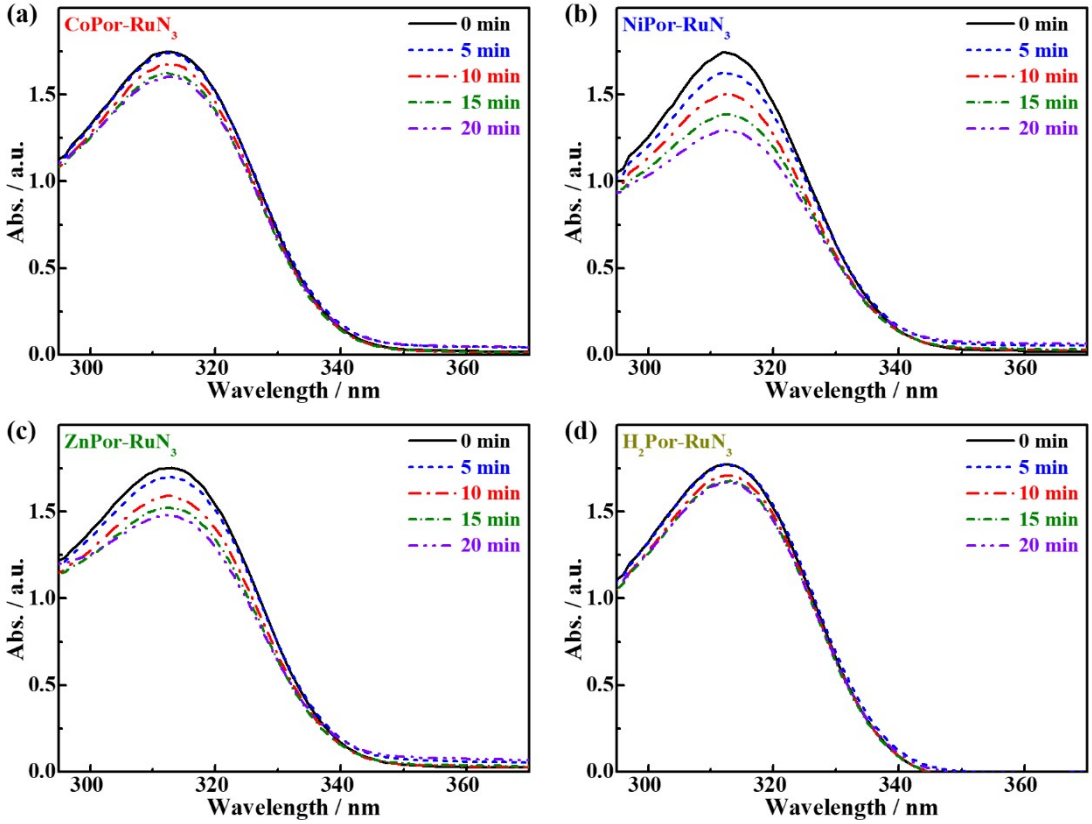

Fig. S15 UV-Vis absorption spectra of the supernatant of various MPor-RuN_3 COP-containing BIH MeCN solutions (0.05 g L^{-1}) under visible light illumination for different periods.

Table S5 Energy band levels of the MPor and RuN_3 monomers.

Sample	$E_{0\text{-}0}$ / eV	E_{HOMO} / V *vs.* NHE	E_{LUMO} / V *vs.* NHE
CoPor	1.94	0.92	-1.02
NiPor	1.96	0.90	-1.06
CuPor	1.97	0.89	-1.08
ZnPor	2.06	0.86	-1.20
RuN_3[27]	2.70	0.62	-2.08

References

1 Y. Xie, Z. Fang, L. Li, H. Yang and T. F. Liu, *ACS Appl. Mater. Interfaces*, 2019, **11**, 27017-27023.

2 C. H. Dai, L. X. Zhong, X. Z. Gong, L. Zeng, C. Xue, S. Z. Li and B. Liu, *Green Chem.*, 2019, **21**, 6606-6610.

3 H. B. Zhang, J. Wei, J. C. Dong, G. G. Liu, L. Shi, P. F. An, G. X. Zhao, J. T. Kong, X. J. Wang, X. G. Meng, J. Zhang and J. H. Ye, *Angew. Chem. Int. Ed.*, 2016, **55**, 14310-14314.

4 K. M. Choi, D. Kim, B. Rungtaweevoranit, C. A. Trickett, J. T. D. Barmanbek, A. S. Alshammari, P. Yang and O. M. Yaghi, *J. Am. Chem. Soc.*, 2017, **139**, 356-362.

5 E. X. Chen, M. Qiu, Y. F. Zhang, Y. S. Zhu, L. Y. Liu, Y. Y. Sun, X. Bu, J. Zhang and Q. Lin, *Adv. Mater.*, 2018, **30,** 1704388.

6 H. Takeda, M. Ohashi, T. Tani, O. Ishitani and S. Inagaki, *Inorg. Chem.*, 2010, **49**, 4554-4559.

7 X. X. Yu, Z. Z. Yang, B. Qiu, S. E. Guo, P. Yang, B. Yu, H. Y. Zhang, Y. F. Zhao, X. Z. Yang, B. X. Han and Z. M. Liu, *Angew. Chem. Int. Ed.*, 2019, **58**, 632-636.

8 M. Lu, J. Liu, Q. Li, M. Zhang, M. Liu, J. L. Wang, D. Q. Yuan and Y. Q. Lan, *Angew. Chem. Int. Ed.*, 2019, **58**, 12392-12397.

9 L. J. Wang, R. L. Wang, X. Zhang, J. L. Mu, Z. Y. Zhou and Z. M. Su, *ChemSusChem*, 2020, **13**, 2973-2980.

10 S. Q. Zhang, L. N. Li, S. G. Zhao, Z. H. Sun and J. H. Luo, *Inorg. Chem.*, 2015, **54**, 8375-8379.

11 G. X. Zhao, H. Pang, G. G. Liu, P. Li, H. M. Liu, H. B. Zhang, L. Shi and J. H. Ye, *Appl. Catal., B*, 2017, **200**, 141-149.

12 G. L. Xu, H. B. Zhang, J. Wei, H. X. Zhang, X. Wu, Y. Li, C. S. Li, J. Zhang and J. H. Ye, *ACS Nano*, 2018, **12**, 5333-5340.

13 Y. L. Jiang, Y. Yu, X. Zhang, M. Weinert, X. L. Song, J. Ai, L. Han and H. H. Fei, *Angew. Chem. Int. Ed.*, 2021, **60**, 17388-17393.

14 L. Shi, T. Wang, H. B. Zhang, K. Chang and J. H. Ye, *Adv. Funct. Mater.*, 2015, **25**, 5360-5367.

15 D. R. Sun, W. J. Liu, Y. H. Fu, Z. X. Fang, F. X. Sun, X. Z. Fu, Y. F. Zhang and Z. H. Li, *Chem. Eur. J.*, 2014, **20**, 4780-4788.

16 F. Guo, Y. P. Wei, S. Q. Wang, X. Y. Zhang, F. M. Wang and W. Y. Sun, *J. Mater. Chem. A*, 2019, **7**, 26490-26495.

17 L. Y. Chen, Y. X. Wang, F. Y. Yu, X. S. Shen and C. Y. Duan, *J. Mater. Chem. A*, 2019, **7**, 11355-11361.

18 Y. P. Wei, Y. Liu, F. Guo, X. Y. Dao and W. Y. Sun, *Dalton Trans.*, 2019, **48**, 8221-8226.

19 H. P. Liang, A. Acharjya, D. A. Anito, S. Vogl, T. X. Wang, A. Thomas and B. H. Han, *ACS Catal.*, 2019, **9**, 3959-3968.

20 Z. W. Fu, X. Y. Wang, A. M. Gardner, X. Wang, S. Y. Chong, G. Neri, A. J. Cowan, L. J. Liu, X. B. Li, A. Vogel, R. Clowes, Matthew Bilton, L. J. Chen, R. S. Sprick and A. I. Cooper, *Chem. Sci.*, 2020, **11**, 543-550.

21 F. M. Wisser, M. Duguet, Q. Perrinet, A. C. Ghosh, M. Alves-Favaro, Y. Mohr, C. Lorentz, E. A. Quadrelli, R. Palkovits, D. Farrusseng, C. Mellot-Draznieks, V. Waele, and J. Canivet, *Angew. Chem. Int. Ed.*, 2020, **59**, 5116-5122.

22 Q. J. Zhi, J. Zhou,W. B. Liu, L. Gong, W. P. Liu, H. Y. Liu, K. Wang and J. Z. Jiang, *Small*, 2022, **18**, 2201314.

23 J. Q. Chen, H. Zhong, H. W. Lv, R. X. Liu and R. H. Wang, *ChemSusChem*, 2021, **14**, 2749-2756.

24 J. Jiang, Y. J. Chen and H. B. Ji, *J. CO_2 Util.*, 2022, **60**, 101972.

25 R. Cheng, C. C. Chung, S. Wang, B. Cao, M. Zhang, C. Chen, Z. Wang, M. Chen, S. Shen and S. P. Feng, *Mater. Today Phys.*, 2021, **17**, 100358.

26 W. J. Wang, K. H. Chen, Z. W. Yang, B. W. Peng and L. N. He, *J. Mater. Chem., A*, 2021, **9**, 16699-16705.

27 S. T. Chen, P. T. Kong, H. Niu, H. R. Liu, X. T. Wang, J. Zhang, R. J. Li, Y. Z. Guo and T. Y. Peng, *Chem. Eng. J.*, 2022, **431**, 133357.